

Crystallization and preliminary X-ray diffraction study of the class A β -lactamase SED-1 and its mutant SED-G238C from *Citrobacter sedlakii*

S. Petrella,^{a†} L. Pernot^{b†} and
W. Sougakoff^{a*}

^aLRMA-Pitié-Salpêtrière, Service de Bactériologie, Faculté de Médecine Pitié-Salpêtrière, Université Pierre et Marie Curie (Paris VI), Paris, France, and ^bLaboratoire de Cristallographie Macromoléculaire, Institut de Biologie Structurale, CEA-CNRS UMR 5075, Grenoble, France

† These authors contributed equally to the work.

Correspondence e-mail:
sougakoff@chups.jussieu.fr

SED-1, a class A β -lactamase from *Citrobacter sedlakii*, is a CTX-M-type extended-spectrum β -lactamase that has the ability to hydrolyze expanded-spectrum cephalosporins such as cefotaxime. SED-1 and a SED mutant in which Gly238 has been replaced by a cysteine, forming a disulfide bridge with the other Cys residue located at position 69 (SED-G238C), have been crystallized. The crystals belong to the monoclinic space group *C2*, with unit-cell parameters $a = 188.09$, $b = 73.65$, $c = 105.41$ Å, $\beta = 121.67^\circ$ for SED-1 and $a = 187.64$, $b = 73.2$, $c = 103.89$ Å, $\beta = 121.89^\circ$ for the SED-G238C mutant. X-ray diffraction data were collected to maximum resolutions of 2.4 Å for SED-1 and 2.0 Å for SED-G238C.

Received 23 July 2003
Accepted 9 October 2003

1. Introduction

A major cause of clinical resistance to β -lactam antibiotics is the production of active-serine class A β -lactamases that catalyze the hydrolysis of the β -lactam ring (Frere *et al.*, 1991; Bush *et al.*, 1995). Among them, new class A β -lactamases capable of hydrolyzing oxyimino-cephalosporins have been selected by the extensive clinical use of the so-called expanded-spectrum cephalosporins (oxyimino-cephalosporins; Matagne *et al.*, 1998; Knox, 1995). These variant enzymes, designated the extended-spectrum β -lactamases (ESBLs), are classified into two groups. The first group (type I) consists of variants of TEM-1 or SHV-1 differing by a few amino-acid substitutions from the two parental enzymes. The second group (type II) includes enzymes that are related neither to TEM-1 nor to SHV-1 (Knox, 1995), such as the CTX-M-type ESBLs which are increasingly on the rise and form the most widespread family of type II ESBLs. They are characterized by an intrinsic efficient hydrolytic activity toward the oxyimino-cephalosporin cefotaxime (CTX; Tzouveleki *et al.*, 2000). A large number of enzymes have been identified in this subgroup, including more than 28 plasmid-encoded CTX-M variants differing from one another by point mutations and also other related enzymes such as TOHO-1 from *Escherichia coli* and K1, the chromosomal enzyme from *Proteus vulgaris* (Ishii *et al.*, 1995; Peduzzi *et al.*, 1994).

To date, only a few structures of ESBLs have been determined, probably because crystals of sufficient quality to allow structure determination are not easily obtained with these enzymes (Raquet *et al.*, 1994; Orenca *et al.*, 2001). Accordingly, all attempts described by Raquet *et al.* (1994) to crystallize TEM-type ESBL variants have failed and Wang *et al.*

(2002) have shown that the enlargement of the active site in TEM ESBLs appears to be at the expense of a decrease in intrinsic stability. Moreover, it has been reported that the wild-type TOHO-1 enzyme has a strong tendency to form twinned crystals (Ibuka *et al.*, 1999) and the crystal structure of TOHO-1, which was determined in 1999, was established from mutants in which the residue Glu166 was replaced by Ala and which were devoid of any significant β -lactamase activity (Ibuka *et al.*, 1999; Shimamura *et al.*, 2002).

Here, we report the purification, crystallization and preliminary X-ray data analysis of the extended-spectrum class A β -lactamase SED-1, which is the chromosome-encoded β -lactamase from *Citrobacter sedlakii*. The enzyme, which preferentially hydrolyzes oxyimino-cephalosporins, belongs to the CTX-M-type ESBLs (Petrella *et al.*, 2001) and shares 71% amino-acid sequence identity with the plasmid-mediated enzyme MEN-1, the first CTX-M-type enzyme described (Bauernfeind *et al.*, 1996). A SED-1 mutant in which the glycine residue in position 238 has been replaced by a cysteine (SED-G238C) has also been crystallized. This mutant was produced with the aim of increasing the internal stability of the protein by linking the two positions 69 and 238 that have previously been shown to form a disulfide bridge in the carbapenem-hydrolyzing class A carbapenemases NMC-A, SME-1 and KPC-1 (Swaren *et al.*, 1998; Sougakoff *et al.*, 2002; Yigit *et al.*, 2001).

2. Methods and results

2.1. Plasmid construction

The *bla* gene encoding SED-1 was obtained by DNA amplification from the clinical strain 2596 of *C. sedlakii*. The PCR was performed

using a reverse primer (5'-TATAAGCTTTACTTTTCCTTCCGTCACAATTTT-3') containing the restriction site *Hind*III (bold) and a forward primer (5'-AGAAGGTTT-CATATGCTTAAGGAACGGTTTCGC-3') designed to anneal at the beginning of the *bla*_{SED-1} gene and containing the restriction site *Nde*I (bold). The PCR product obtained using these two primers was purified from agarose gel with the Prepagen kit (Bio-Rad) and was first cloned in a pMOSblue vector. The insert containing the *bla*_{SED-1} gene was then recovered by digestion with *Hind*III and *Nde*I and was ligated by T4 DNA ligase into the *Hind*III- and *Nde*I-restricted sites of the pET29a plasmid. The recombinant plasmid DNA was introduced by transformation into *E. coli* Top10 competent cells. For the SED-G238C mutant, site-directed mutagenesis experiments were performed by PCR with the 'Megaprimer' method (Barik & Galinski, 1991). The mutation was introduced using the mutagenic primer 5'-GATAAAACCGGGCGTGTGATTACGGC-3' containing the two mutations (in bold) determining the Cys residue in position 238. The mutated gene was cloned into pET-29a following the procedure described above for the wild-type gene. The clones harbouring the recombinant plasmids (wild-type and mutant) were used for protein expression. It is worth noting here that the two proteins, SED-1 and the SED-G238C mutant, were produced without a His tag because the presence of a six-His tag resulted in precipitation of the proteins in most of the crystallization conditions tested.

2.2. Protein expression, purification and crystallization

For the crystallization experiments, the wild-type SED-1 enzyme and its mutant G238C were purified from a culture of 6 × 500 ml LB. Protein expression was induced by adding 0.4 mM IPTG to the culture. Bacterial cells were pelleted, resuspended in 240 ml 40 mM Tris pH 7.8 and lysed by ultrasonic treatment. The suspension was clarified by centrifugation at 38 000g at 277 K. The nucleic acids contained in the supernatant were precipitated by adding spermine (0.2 M) at 277 K, followed by 10 min of centrifugation at 12 000g and 60 min at 48 000g. The supernatant was then dialysed overnight against 3 140 mM Tris pH 7.8. After an additional centrifugation at 12 000g for 30 min, the supernatant was applied onto a 2.5 × 10 cm Q Sepharose Fast Flow column (Pharmacia Co. Ltd, Sweden) previously equilibrated with dialysis buffer. β-Lactamase activity was detected in the

unadsorbed fraction with the chromogenic cephalosporin nitrocefin (O'Callaghan *et al.*, 1972). The active fractions were pooled, dialysed overnight at 277 K against 21 40 mM HEPES [N-(2-hydroxyethylpiperazine)-N'-ethanesulfonic acid] pH 7.2 and loaded onto a Bioscale S cation-exchange column (Bio-Rad) previously equilibrated with dialysis buffer. The protein was eluted with a linear gradient of 0–1 M NaCl in 40 mM HEPES pH 7.2. Active fractions were pooled and loaded onto a gel-filtration Superdex 75 (Pharmacia Co. Ltd, Sweden) column previously equilibrated with 20 mM Tris pH 7.8. Analysis of the elution profiles in the purification process showed that the wild-type SED-1 enzyme and the G238C mutant produced a single β-lactamase peak at each step of purification (data not shown). The enzyme was finally concentrated using Microcon 3 (Millipore) to a final concentration of 10 mg ml⁻¹.

The crystallization experiments were carried out at 291 K using the hanging-drop vapour-diffusion technique. Clear Strategy Screen 1 and 2 kits (Molecular Dimensions Ltd) were used for initial trials. 6 μl drops made by mixing an equal volume of protein solution and reservoir solution were equilibrated against 500 μl reservoir solution. For SED-1, crystals were obtained from seven of

the 48 trials tested. The preliminary conditions that gave the best results, *i.e.* pH 6.5, 25% PEG 2 K MME and 200 mM KBr (Clear Strategy Screen 1, condition 4) or 15% PEG 4K and 200 mM KSCN (Clear Strategy Screen 1, condition 11), yielded needles of poor quality (Fig. 1*a*). Optimization was undertaken using different concentrations of KSCN combined with PEGs of different sizes in the pH range 6.5–8.5. Well shaped crystals of SED-1 (0.6 × 0.06 × 0.04 mm) were finally obtained using 35% PEG 10K, 200 mM KSCN, 100 mM Tris-HCl pH 8.5 (Fig. 1*b*). For the mutant protein SED-G238C, poorly shaped and twinned crystals were obtained using 25% PEG 2K MME and 100 mM KSCN pH 6.5–8.5 (Fig. 1*c*). The number of crystals was reduced and the size of the crystals was increased by using higher concentrations of KSCN. Similar results were obtained when higher concentrations of PEG were used. Finally, crystals of SED-G238C suitable for X-ray data collection (0.7 × 0.14 × 0.07 mm) were obtained using 35% PEG 2K MME, 200 mM KSCN, 100 mM sodium cacodylate at pH 6.5 (Fig. 1*d*).

2.3. Data collection

Prior to data collection, crystals were transferred into a stabilizing solution

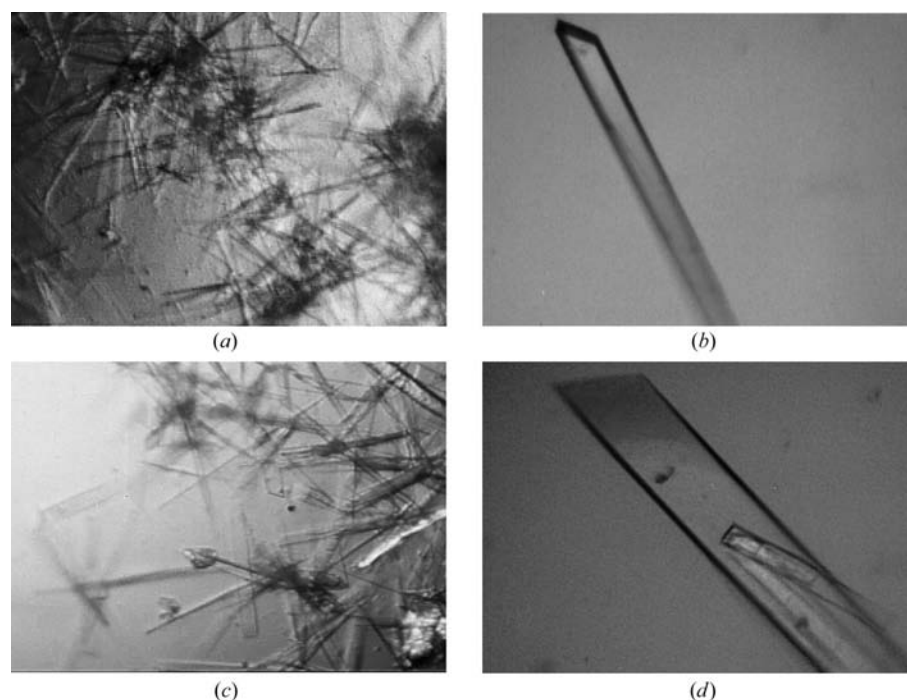


Figure 1

Crystals of the β-lactamase SED-1 (*a* and *b*) and of the G238C mutant of SED-1 (*c* and *d*) grown by vapour diffusion using the hanging-drop method. The composition of the reservoir solution was (*a*) 15% polyethylene glycol 4000 pH 6.5, 0.2 M potassium thiocyanate, (*b*) 35% polyethylene glycol 10 000 pH 8.5, 0.2 M potassium thiocyanate, (*c*) 25% polyethylene glycol MME 2000, 0.1 M sodium cacodylate pH 6.5, 0.1 M potassium thiocyanate and (*d*) 35% polyethylene glycol MME 2000, 0.2 M potassium thiocyanate, 0.1 M sodium cacodylate pH 6.5. Crystals shown in the four parts are on the same scale.

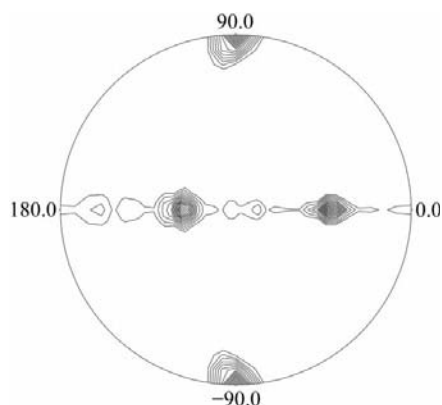


Figure 2

Stereographic projection of the self-rotation function calculated from the SED-G238C data set using the structure-factor amplitudes in the resolution range 17–3 Å and an integration radius of 30 Å. The orthogonalization code places a parallel to x , c^* parallel to z and b parallel to y . The angle κ is the rotation angle around the axis, the angle θ is the angle between the rotation axis and z and φ is the angle in the xy plane between x and the projection of the rotation axis. The section displayed is for $\kappa = 180^\circ$. Contours start at the 2σ level and increase in 5σ intervals.

consisting of mother liquor supplemented with 20% PEG 400. X-ray diffraction data sets for SED-1 and the mutant SED-G238C were collected on beamline BM14 at the European Synchrotron Radiation Facility (Grenoble, France) equipped with a MAR CCD detector and tuned at wavelengths close to 0.9 Å. Each data set was obtained from a single crystal. Raw diffraction images were indexed and integrated with *MOSFLM* v.6.2.2 (Leslie, 2002). Crystals of both molecules belong to space group $C2$ and have fairly similar unit-cell parameters, suggesting that they have identical crystal packings. Data scaling, merging and reduc-

Table 1
Data-collection statistics.

Values in parentheses represent the values for the highest resolution shell (2.0–2.1 Å for SED-G238C and 2.53–2.4 Å for SED-1).

Data set	SED-G238C	SED-1
Space group	$C2$	$C2$
Unit-cell parameters		
a (Å)	187.6	188.0
b (Å)	73.2	73.6
c (Å)	103.8	105.4
β (°)	121.8	121.6
Wavelength (Å)	0.999	0.983
Crystal-to-detector distance (mm)	140	120
Angular increment (° per image)	1	0.7
Resolution limits (Å)	16–2.0	31–2.4
No. measured reflections	283335	107585
No. unique reflections	80352	42773
Multiplicity	3.5 (2.3)	2.5 (2.3)
Completeness (%)	99.3 (96.4)	89.4 (81.8)
$\langle I/\sigma(I) \rangle$	8.7 (2.0)	7.21 (3.65)
R_{merge}^\dagger (%)	10.2 (33.0)	9.1 (16.1)

$^\dagger R_{\text{merge}} = \frac{\sum_{hkl} \sum_i |I(hkl, i) - \langle I(hkl) \rangle|}{\sum_{hkl} \sum_i I(hkl, i)}$, where $I(hkl, i)$ represents the i th measurement of the intensity of the hkl reflection and its symmetry equivalent and $\langle I(hkl) \rangle$ is the average intensity of the hkl reflection.

tion were carried out with programs from the *CCP4* suite (Collaborative Computational Project, Number 4, 1994). Relevant statistics are given in Table 1.

With a molecular weight of 29 kDa per monomer, reasonable values of the Matthews coefficient V_M (Matthews, 1968) were obtained considering four ($V_M = 2.58 \text{ \AA}^3 \text{ Da}^{-1}$) or three ($V_M = 3.44 \text{ \AA}^3 \text{ Da}^{-1}$) monomers in the asymmetric unit. These values are in the normal range for globular proteins and correspond to solvent contents of 52 and 64%, respectively.

The presence of non-crystallographic symmetry elements was searched for by calculating a self-rotation function with the

program *MOLREP* (Vagin & Teplyakov, 1997) from the SED-G238C data set (the self-rotation function for SED-1 produced identical results). In the $\kappa = 180^\circ$ section, three peaks were observed (Fig. 2). The peak at $\theta = 90, \varphi = 90$ and $\theta = 90, \varphi = -90^\circ$ represents the crystallographic twofold axis of the crystal, which is parallel to the b axis. The second peak at $\theta = 56.5, \varphi = 0^\circ$ corresponds to a non-crystallographic twofold axis, while the third peak at $\theta = 33.5, \varphi = 180^\circ$ is related to a second non-crystallographic twofold axis generated by the non-crystallographic twofold axis and the crystallographic twofold axis.

In the native Patterson map calculated at 2.0 Å resolution with the program *FFT* from the *CCP4* suite (Fig. 3), we observed a strong non-origin peak at position (0.375, 0, 0.877) whose height corresponded to 15% of the height of the origin peak. This peak was linked to a non-crystallographic symmetry defined by a pure translation. Alternatively, the fact that the non-origin peak in the Patterson map is located in the $y = 0$ section suggests the presence of a non-crystallographic twofold axis parallel to the crystallographic twofold axis (*i.e.* parallel to b). This would be compatible with a tetramer of point-group symmetry $222 (D_2)$ in the asymmetric unit.

In conclusion, we have established crystallization conditions that allow X-ray crystallographic analysis of the ESBL SED-1. Attempts to solve the structure of SED-1 and its mutant SED-G238C by the molecular-replacement approach are in progress.

We thank Philippe Carpentier for assistance in data collection at beamline BM-14 at the ESRF. We thank Guillaume Gautier for technical assistance. This work was supported by the Programme de Recherche Fondamentale en Microbiologie et Maladies Infectieuses et Parasitaires (MENRT grant 'Réseau de Recherche sur les β -lactamases') and by the Institut National de la Santé et de la Recherche Médicale (Grant EMI 0004). Stéphanie Petrella is a fellow of the Fondation pour la Recherche Médicale.

References

- Barik, S. & Galinski, M. S. (1991). *Biotechniques*, **10**, 489–490.
- Bauernfeind, A., Stemplinger, I., Jungwirth, R., Ernst, S. & Casellas, J. M. (1996). *Antimicrob. Agents Chemother.* **40**, 509–513.
- Bush, K., Jacoby, G. A. & Medeiros, A. A. (1995). *Antimicrob. Agents Chemother.* **39**, 1211–1233.
- Collaborative Computational Project, Number 4 (1994). *Acta Cryst.* **D50**, 760–766.

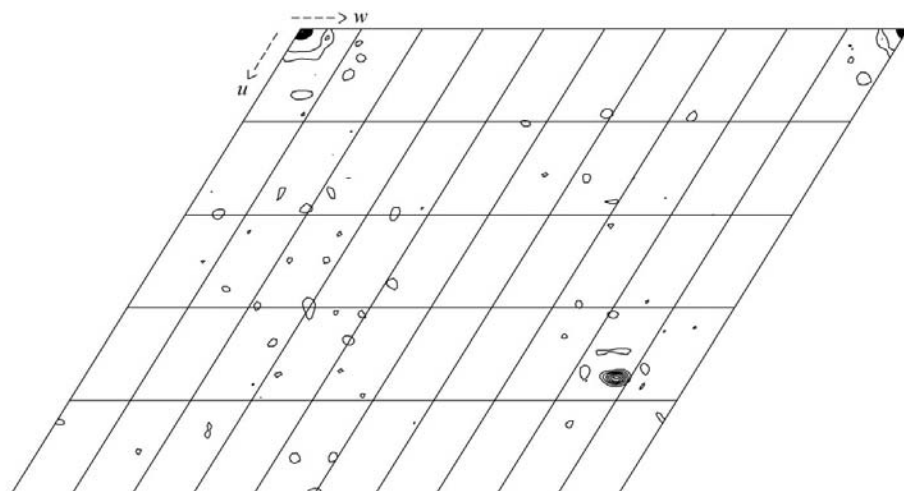


Figure 3

Navite Patterson map of SED-G238C at 2.0 Å resolution. The asymmetric unit of the $y = 0$ section is shown. The contours start at the 2σ level and increase in 5σ intervals.

- Frere, J. M., Joris, B., Granier, B., Matagne, A., Jacob, F. & Bourguignon-Bellefroid, C. (1991). *Res. Microbiol.* **142**, 705–710.
- Ibuka, A., Taguchi, A., Ishiguro, M., Fushinobu, S., Ishii, Y., Kamitori, S., Okuyama, K., Yamaguchi, K., Konno, M. & Matsuzawa, H. (1999). *J. Mol. Biol.* **285**, 2079–2087.
- Ishii, Y., Ohno, A., Taguchi, H., Imajo, S., Ishiguro, M. & Matsuzawa, H. (1995). *Antimicrob. Agents Chemother.* **39**, 2269–2275.
- Knox, J. R. (1995). *Antimicrob. Agents Chemother.* **39**, 2593–2601.
- Leslie, A. G. W. (2002). *MOSFLM version 6.2.2*. MRC Laboratory of Molecular Biology, Cambridge, England.
- Matagne, A., Lamotte-Brasseur, J. & Frère, J. M. (1998). *Biochem. J.* **330**, 581–598.
- Matthews, B. W. (1968). *J. Mol. Biol.* **33**, 491–497.
- O'Callaghan, C. H., Morris, A., Kirby, S. M. & Shingler, A. H. (1972). *Antimicrob. Agents Chemother.* **1**, 283–288.
- Orencia, M. C., Yoon, J. S., Ness, J. E., Stemmer, W. P. & Stevens, R. C. (2001). *Nature Struct. Biol.* **8**, 238–242.
- Peduzzi, J., Reynaud, A., Baron, P., Barthelemy, M. & Labia, R. (1994). *Biochim. Biophys. Acta*, **1207**, 31–39.
- Petrella, S., Clermont, D., Casin, I., Jarlier, V. & Sougakoff, W. (2001). *Antimicrob. Agents Chemother.* **45**, 2287–2298.
- Raquet, X., Lamotte-Brasseur, J., Fonze, E., Goussard, S., Courvalin, P. & Frere, J. M. (1994). *J. Mol. Biol.* **244**, 625–639.
- Shimamura, T., Ibuka, A., Fushinobu, S., Wakagi, T., Ishiguro, M., Ishii, Y. & Matsuzawa, H. (2002). *J. Biol. Chem.* **277**, 46601–46608.
- Sougakoff, W., L'Hermite, G., Pernot, L., Naas, T., Guillet, V., Nordmann, P., Jarlier, V. & Deletre, J. (2002). *Acta Cryst.* **D58**, 267–274.
- Swaren, P., Maveyraud, L., Raquet, X., Cabantous, S., Duez, C., Pedelacq, J. D., Mariotte-Boyer, S., Mourey, L., Labia, R., Nicolas-Chanoine, M. H., Nordmann, P., Frere, J. M. & Samama, J. P. (1998). *J. Biol. Chem.* **273**, 26714–26721.
- Tzouveleakis, L. S., Tzelepi, E., Tassios, P. T. & Legakis, N. J. (2000). *Int. J. Antimicrob. Agents*, **14**, 137–142.
- Vagin, A. A. & Teplyakov, A. (1997). *J. Appl. Cryst.* **30**, 1022–1025.
- Wang, X., Minasov, G. & Shoichet, B. K. (2002). *J. Mol. Biol.* **320**, 85–95.
- Yigit, H., Queenan, A. M., Anderson, G. J., Domenech-Sanchez, A., Biddle, J. W., Steward, C. D., Alberti, S., Bush, K. & Tenover, F. C. (2001). *Antimicrob. Agents Chemother.* **45**, 1151–1161.